Solid State Communications 205 (2015) 33–38

Contents lists available at ScienceDirect

Solid State Communications

journal homepage: www.elsevier.com/locate/ssc

Linear and nonlinear properties of ultraviolet fluorine crystal: A first-principles study

Xiaole Zhang [a], Shijie Liu [a], Xianfeng Chen [a,*], Weidong Luo [b,c]

[a] Department of Physics and Astronomy, State Key Laboratory of Advanced Optical Communication Systems and Networks, Shanghai Jiao Tong University, Shanghai 200240, PR China

[b] Key Laboratory of Artificial Structures and Quantum Control (Ministry of Education), Department of Physics and Astronomy, Shanghai Jiao Tong University, Shanghai 200240, PR China

[c] Institute of Natural Sciences, Shanghai Jiao Tong University, Shanghai 200240, PR China

ARTICLE INFO

Article history:
Received 20 October 2014
Received in revised form
18 December 2014
Accepted 31 December 2014
by H. Akai
Available online 13 January 2015

Keywords:
A. Ferroelectrics
D. Optical properties
D. Electronic band structure

ABSTRACT

The electronic structure and optical properties of Deep Ultraviolet (DUV) nonlinear optical crystal $BaMgF_4$ and $KBe_2BO_3F_2$ have been studied in the framework of many-body perturbation theory as well as hybrid functionals. For the electronic properties, the hybrid functionals method makes significant improvement on description of electronic band gap for both crystals. However, the results still underestimate the band gap comparing with the *GW* results. By considering the self-energy of electrons, electronic band gap and the optical band gap are both described well comparing with the experimental results, which is crucial for prediction the performance of DUV crystals in the DUV region. In addition to the remarkable self-energy effect, the macroscopic dielectric function and related optical properties, such as refractive index $n(\omega)$, excitation coefficient $k(\omega)$, absorption coefficient $\alpha(\omega)$, energy-loss function $L(\omega)$, and reflectivity $R(\omega)$ have been calculated by solving Bethe–Salpeter equation (BSE). By comparing the RPA results and BSE results, we found that the excitonic effects play an important role in description of optical properties, which is absence in the previous work. Furthermore, taking advantage of $2n+1$ theorem, the nonlinear optical susceptibility have been calculated as well. As all key factors that determine the performance of DUV nonlinear crystals have been addressed theoretically, our present work pave the way using first-principle theory to assist the crystal engineering for other candidates of DUV nonlinear optical crystal.

© 2015 Elsevier Ltd. All rights reserved.

1. Introduction

Deep-ultraviolet (DUV) laser below 200 nm attract great interest in photoemission spectroscopy, laser spectroscopy, semiconductor photolithography, micromachining and photochemical synthesis [10,27]. DUV all-solid-state laser through direct frequency-doubled present great application merits and markets for its simplicity, stability, narrower spectral bandwidth, better beam quality and easier maintenance compared to other DUV coherent light devices.

There are several nonlinear optical (NLO) crystals, such as BBO, CLBO and LBO can produce DUV laser by nonlinear frequency conversion [17,19]. However, for DUV region below 200 nm, they can only be used with sum-frequency mixing, which makes the laser system complex and efficiency low. So the ferroelectric fluoride named $BaMgF_4$ and $KBe_2BO_3F_2$ which show a wide transparency range and good nonlinear optical properties attract great attention [26,3]. Their cut-off wavelength in the DUV side is up to 125 nm and 150 nm respectively [21,8]. In the last decade, both of the two fluoride had been investigated by theoretical and experimental methods. Theoretically, Lin et al. performed the density functional theory (DFT) with both local density approximation (LDA) and generalized gradient approximation (GGA) to investigate the crystal structure, electronic properties, linear and nonlinear optical properties of the two crystals [12,7,11,9]. Moreover, using the anionic group theory, the mechanism of the linear and nonlinear optical effects was elucidated as well. Experimentally, Buchter et al. demonstrated the periodically reversed ferroelectric domains of $BaMgF_4$, which make it theoretically possible to produce 125 nm DUV radiation through the quasi-phase-matching (QPM) method [1]. Recently, Chen et al. measured the second, third-order nonlinear optical characterizations as well as self-phase modulation of $BaMgF_4$ through Z-scan method [4].

Although the $BaMgF_4$ and KBBF are good candidates for the applications of DUV all-solid state laser, both of them has their own *pro and cons*. For KBBF, it is too fragile to grow because of its

* Corresponding author.
E-mail address: xfchen@sjtu.edu.cn (X. Chen).

http://dx.doi.org/10.1016/j.ssc.2014.12.023
0038-1098/© 2015 Elsevier Ltd. All rights reserved.

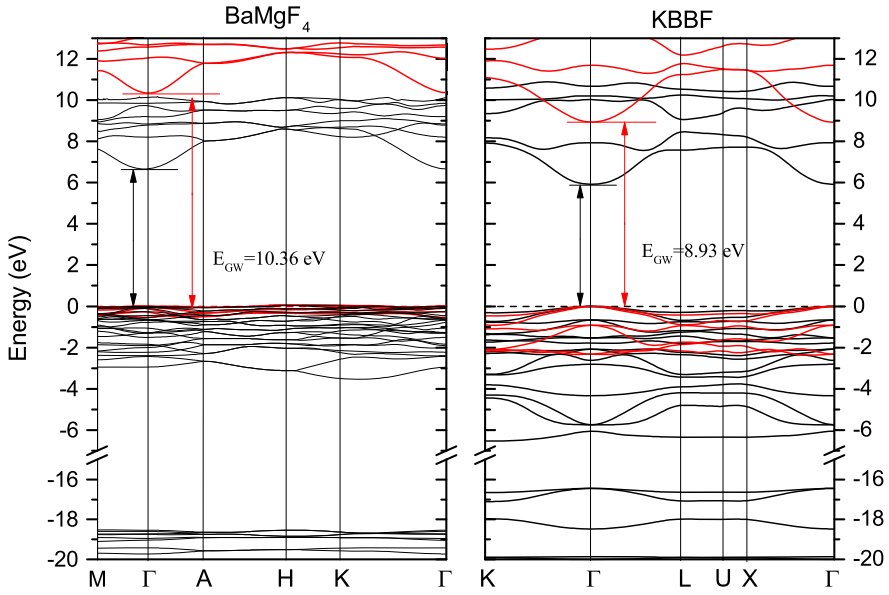

Fig. 1. (Color online) Band structure of $BaMg_4$ (a) and KBBF (b) along; the high symmetry line; the solid black lines are LDA results and the solid red lines are *GW* results. Fermi level is set at the top of the valence bands for both LDA and *GW* results.

Table 1
Calculated fundamental bandgaps (given in eV) of $BaMgF_4$ and $KBe_2BO_3F_2$ comparing with other calculation.

Crystals	Electronic band gap		
	DFT	HSE06	*GW*
$BaMgF_4$	6.55(6.66)	9.50	10.36
$KBe_2BO_3F_2$	5.92(5.66)	8.92	8.93

strong layer tendency along the *z*-axis, make it hard to grow thicker then even 2 mm [2]. Besides, the composition used to grow the crystal is toxic. For $BaMgF_4$, the birefringence of this crystal is too small (0.02) to directly archive the birefringent phase matching in the DUV region. Since the difficulty of crystal growing and the limitations of the experiment, theoretical investigation could be a promising tool to assist the crystal engineering to find candidates possess more attractive properties. However, the 'bandgap problem' due to the absence of self-interaction effect as well as the 'independent-electron picture' of random-phase approximation for calculating linear optical properties, make the DFT-level calculations not accurate enough to predict the electronic gap nor optical gap for new DUV nonlinear optical crystals [23,20,18]. For the 'bandgap problem', there are three scheme to overcome it, which are Hubuardd U method, hybrid functionals and *GW* corrections. The first one is most efficient but only suitable for the localized orbitals such as *d*, *f* electrons of the system; the second one is also system dependent and the determination of mixing factor β make this scheme is not 'purely' *ab initio*; and the last one is more 'physical' than above two methods, however, the consumption of the computation is unbearable for big systems. For the linear optical calculation, the independent particle approximation, known as RPA, make the theory not suitable for describing the process between N and $N+1(N-1)$ systems. As a result, the *GW* method and corresponding *BSE* method become natural for calculating the properties of such materials. To the best of our knowledge, there is no systematical calculations of electronic and optical properties based on many-body theory for the existing two wide-gap nonlinear optical crystals. Therefor, in this work, the calculations based on many-body theory were performed for the electronic and optical properties of the two crystals. The hybrid functionals calculations

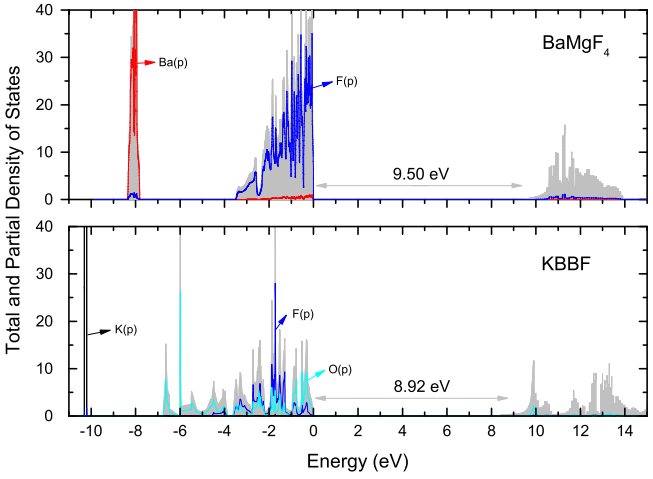

Fig. 2. (Color online) Total and partial density of states of $BaMg_4$ and KBBF.

were performed as well for comparison reason. This study not only confirm the validation of the many body theory on description for the DUV optical crystal, but also give a scenario, which is independent of experimental measurements, to further assisting the searching for new prominent DUV nonlinear optical crystals.

2. Computational details

The calculations are performed within density functional theory, using a plane waves pseudopotentials method as implemented in the ABINIT package [5]. The exchange-correlation energy functional is evaluated within the local density approximation (LDA) as parametrized by Perdew and Wang [16]. The all-electron potentials are replaced by norm-conserving pseudopotentials generated according to the Troullier–Martins scheme [22]. With Ba(5 s,5p,6 s), Mg(3 s), F(2 s,2p) electrons are considered as valence states for $BaMgF_4$ and K(3 s), B(3 s), Be(3 s) and O(3 s) electrons for KBBF. The wave functions are expanded up to a kinetic energy cutoff of 50 Hartrees. Integrals over the Brillouin zone (BZ) are approximated by sums on a $6\times6\times6$ Monkhorst–Pack mesh of special *k*-points [14]. The second-order

nonlinear optical susceptibilities and EO coefficients are obtained within a nonlinear response formalism taking advantage of the $2n+1$ theorem [25,24]. Starting from the LDA wave functions and Coulomb screening, we calculate the QP energies ("true" single-particle excitation energies) within the *GW* approximation for the electron self-energy operator Σ by solving the Dyson equation [15]:

$$\left[-\delta^2/2+V_{ext}+V_{Hartree}+\sum(E^{qp}_{nk})\right]\Phi^{qp}_{nk}=E^{qp}_{nk}\Phi^{qp}_{nk}. \quad (1)$$

The equation is solved nonself-consistently, i.e. within the G_0W_0 approximation, leading to $\Sigma=iG_0W_0$. The reducible response function is obtained with random phase approximation and the dynamical screening effects in self-energy are taken into account through the generalized plasmon pole model. The optical absorption spectrum, which is directly associated with the imaginary part of the macroscopic dielectric function, is defined in terms of microscopic inverse dielectric function. The coupled excitonic effect and absorption spectrum are calculated by solving the Bethe–Salpeter equation through standard Tamm–Dancoff approximation. Calculations including many-body effects are performed using the YAMBO program suite [13]. Specifically, for the GW and BSE calculations, we used 200 bands for the expansion of Green's function, exchange components within 40 Ry and correlation components within 10 Ry are included in our calculation of self-energy and dielectric matrix. Converged studies for each parameters have been performed carefully. All the calculations are based on the same *k*-point sampling as the DFT level.

3. Results and discussion

3.1. Electronic properties

First, we calculate the band structure for both crystals by using DFT and G_0W_0 approach. The calculated QP band structure for both crystals comparing with the results of DFT is shown in Fig. 1. At the DFT-LDA level, as shown in Fig. 1 and Table 1, both $BaMgF_4$ and KBBF demonstrates direct band gap located at Γ point, with values of 6.55 eV and 5.92 eV respectively, which is in good agreement with previous calculations [12,7,11,9]. However, it is well known that DFT generally underestimates the band gap due to the absence of self-energy effect. In order to improve the theoretical evaluation of the band gap, we use the *GW* approximation to describe the band structures of both crystals. As shown in Fig. 1 with solid blue lines, after considering the *e–e* self-energy effects, the band gap of $BaMgF_4$ and KBBF are strongly enlarged to 10.36 eV and 8.93 eV respectively. From the *GW* band structures, the corrections are *k*-point dependent which indicate that there is no simple "*scissor rule*" for the band structure because the QP corrections manifest a complicated momentum and energy dependence.

It should be pointed out that the band gaps calculated at the *electronic* level are comparable with the results obtained from photoemission and inverse-photoemission spectroscopy instead of the absorption spectra. This is because the *e–h* Coulomb attraction involved in optical excitations is not considered in the calculation of single-particle spectra. As a consequence, it is inappropriate to verify the calculated *electronic* band gap with the *optical* gap extrapolated from the absorption spectrum as a reference. The *optical* gap should be calculated by the BSE, which will be discussed later.

Besides the *GW* corrections, the calculations based on the hybrid functionals are performed as well for comparison. Since the hybrid functionals only calculate the exact Hartree-Fock term and use the existing DFT screen interaction, the consumption of calculation time will reduce significantly at the cost of introducing more empirical parameters. In this work, we used the screen hybrid functional of Heyd, Scuseria, and Ernzerhof (HSE06) [6] to calculate density of states for both crystals. The parameter used in HSE06 is a fixed HF:DFT mixing ratio of 25:75 and a screening parameter of 0.2 $Å^{-1}$, which was shown to be successful in describing not just the band gap but also the ground-state properties of a wide range of materials. The calculated results are shown in Fig. 2. The band gaps of $BaMgF_4$ and KBBF are 9.50 eV and 8.92 eV, which are relatively small comparing with the *GW* results. From Fig. 2, the top of the valence bands of $BaMgF_4$ is mainly composed of the 2*p* orbital of F atoms, while hybridized Ba 3*d* and F 2*p* orbitals predominately contribute to the bottom of the conduction bands. For KBBF, the hybridized F 2*p* and O 2*p* orbitals dominate the main characteristics of the top valence bands, while the hybridized F 3*d* and O 3*d* orbitals determined the characteristics of the bottom conduction bands. As for both crystals, the bands near the Fermi level are relatively flat indicating localized electrons, which is a consequence of the potential inhomogeneity within the crystals.

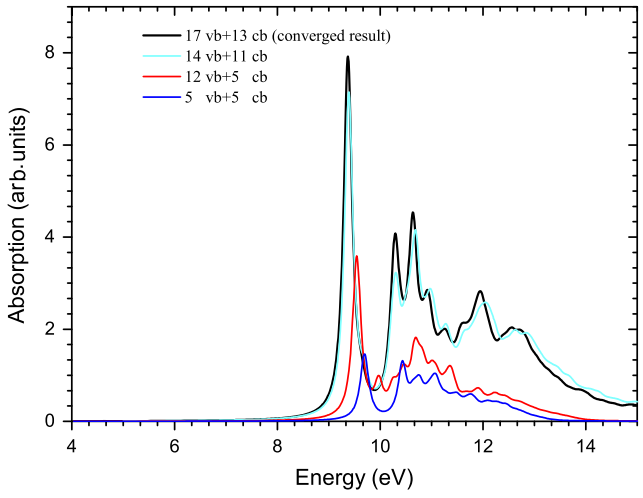

Fig. 3. (Color online) Converged study of the absorption spectrum of $BaMgF_4$ on the bands used to construct the *e–h* basis. vb is abbreviation of valence band; cb is abbreviation of conduction band.

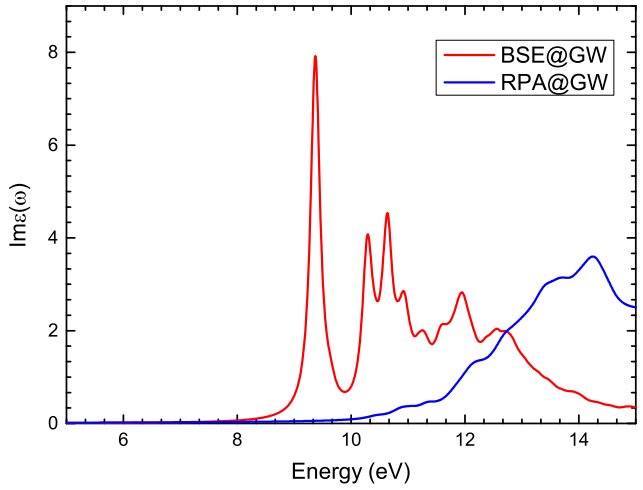

Fig. 4. (Color online) Imaginary part of macroscopic dielectric function ϵ_M for light polarization parallel to [100] direction calculated with (solid red line) and without (solid blue line) *e–h* interactions. A Lorentzian broadening of 0.1 eV was adopted.

3.2. Linear optical properties

The optical absorption spectra, which are directly associated with the imaginary part of the macroscopic dielectric function ϵ_M, were

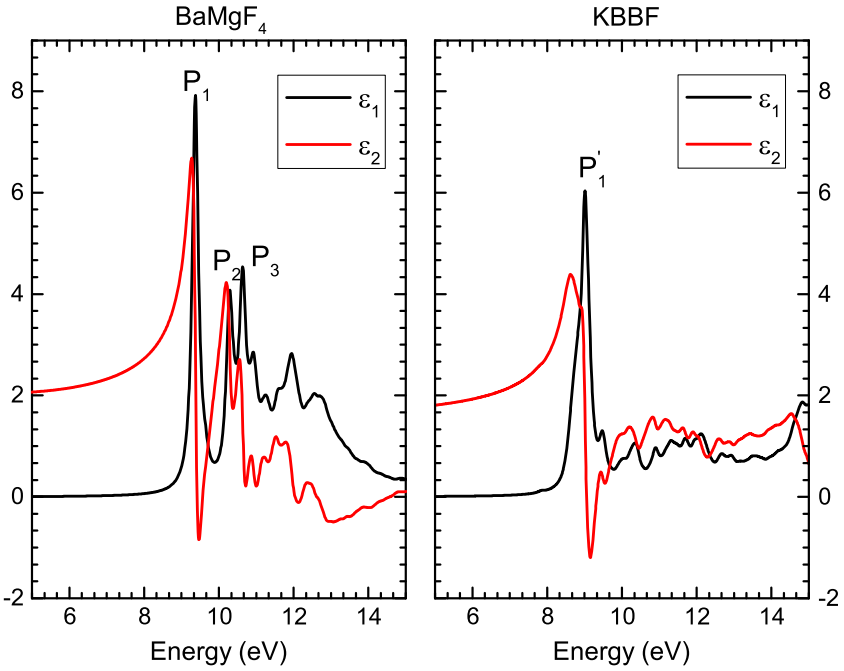

Fig. 5. (Color online) Real and imaginary part of macroscopic dielectric function ϵ_M for light polarization parallel to [100] direction.

calculated for both crystals by using random-phase approximation based on GW corrected eigenstate level (RPA@GW) and by solving Bethe–Salpeter equation based on GW corrected eigenstate level (BSE@GW). For RPA@GW, the crystal local field effects (LFE) are already taken into account. The LFE for both crystals only cause slight modification to the overall profile of the spectra. For BSE@GW, since the reliability of BSE result is based on the size of the *e–h* basis set that include in the calculation, we conduct the convergence study of *e–h* basis set for both crystal, as shown in Fig. 3. Begin with 5 valence bands and 5 conduction bands, the oscillator strength is relatively small because of the absence of possible excitations. With increasing the bands involved in calculations, the result obtained using 17 valence bands and 12 conduction bands is converged for $BaMgF_4$.

With the converged parameters, the optical absorption spectra of both crystals calculated with (BSE@GW) and without (RPA@GW) *e–h* interaction are shown in Fig. 4. Since the differences of dielectric function between different orientations are small, here we only present the optical spectra parallel to [100] direction. The optical spectrum at the RPA@GW level demonstrates that the direct optical transitions are significantly blue-shifted compare to the experimental results, which also indicate the failure of the "*scissor rule*" for the optical properties calculations. As shown in Fig. 4, dramatic changes occur when *e–h* Coulomb interactions are included in the calculations. Optical absorption of both crystal is greatly modified and strongly bound excitation states well below the onset of single-particle transition continuum are indicated. This prominent variation from the single-particle spectrum reveals a weight redistribution of the oscillator strength, most of which is collected by the strongly bound excitonic states. Therefore, there is an obvious cancellation effect between the band-gap opening due to the QP corrections and the redshift of optical absorption due to the excitonic effects.

The spectrum of $\epsilon_2(\omega)$ of $BaMgF_4$ and KBBF in Fig. 5 indicates that the threshold energy of the dielectric function occurs at around 9.26 eV and 7.84 eV, respectively. This corresponds to the optical transition between the valence bands and conduction bands, which is known as the fundamental absorption edge, or optical gap. Our results are in good agreement with experimental data [12,7,11,9], which is 9.28 eV and 7.98 eV. For $BaMgF_4$, with increasing the energy, the absorptive part of $\epsilon_2(\omega)$ exhibits three predominant peaks locating at 9.38 eV, 10.31 eV and 10.68 eV. The first peak is in nature of transitions from the third top valence band to the first conduction band at the Γ point; the second peak is constructed by the multibands transitions from the top valence bands to the first conduction band at the Γ point; the third peak is mainly originated from the transition from the top valence band to the third conduction band. For the KBBF, there is only one main peak located at 9.01 eV. The peak is mainly originated from the transition from the multibands transitions from the top valence bands to the first conduction band, which is similar with the second peak in $BaMgF_4$ case.

Based on the real and imaginary part of ϵ_M we calculated, based on BSE@GW, as shown in Fig. 5, we can straightforwardly calculate all the frequency-dependent optical spectra (e.g., refractive index $n(\omega)$, excitation coefficient $k(\omega)$, absorption coefficient $\alpha(\omega)$, energy-loss function $L(\omega)$, and reflectivity $R(\omega)$ from the real $\epsilon_1(\omega)$ and the imaginary $\epsilon_2(\omega)$ parts) by using the following equation:

$$n(\omega)=\left[\frac{\sqrt{\epsilon_1^2+\epsilon_2^2}+\epsilon_1}{2}\right]^{1/2}, \tag{2}$$

$$k(\omega)=\left[\frac{\sqrt{\epsilon_1^2+\epsilon_2^2}-\epsilon_1}{2}\right]^{1/2}, \tag{3}$$

$$\alpha(\omega)=\sqrt{2}\omega\left[\frac{\sqrt{\epsilon_1^2+\epsilon_2^2}-\epsilon_1}{2}\right]^{1/2}, \tag{4}$$

$$L(\omega)=\frac{\epsilon_2}{\epsilon_1^2+\epsilon_2^2}, \tag{5}$$

$$R(\omega)=\frac{(n-1)^2+k^2}{(n+1)^2+k^2}. \tag{6}$$

The related frequency-dependent optical properties are plotted in Fig. 6 which can be directly compared with experimental results if there is any.

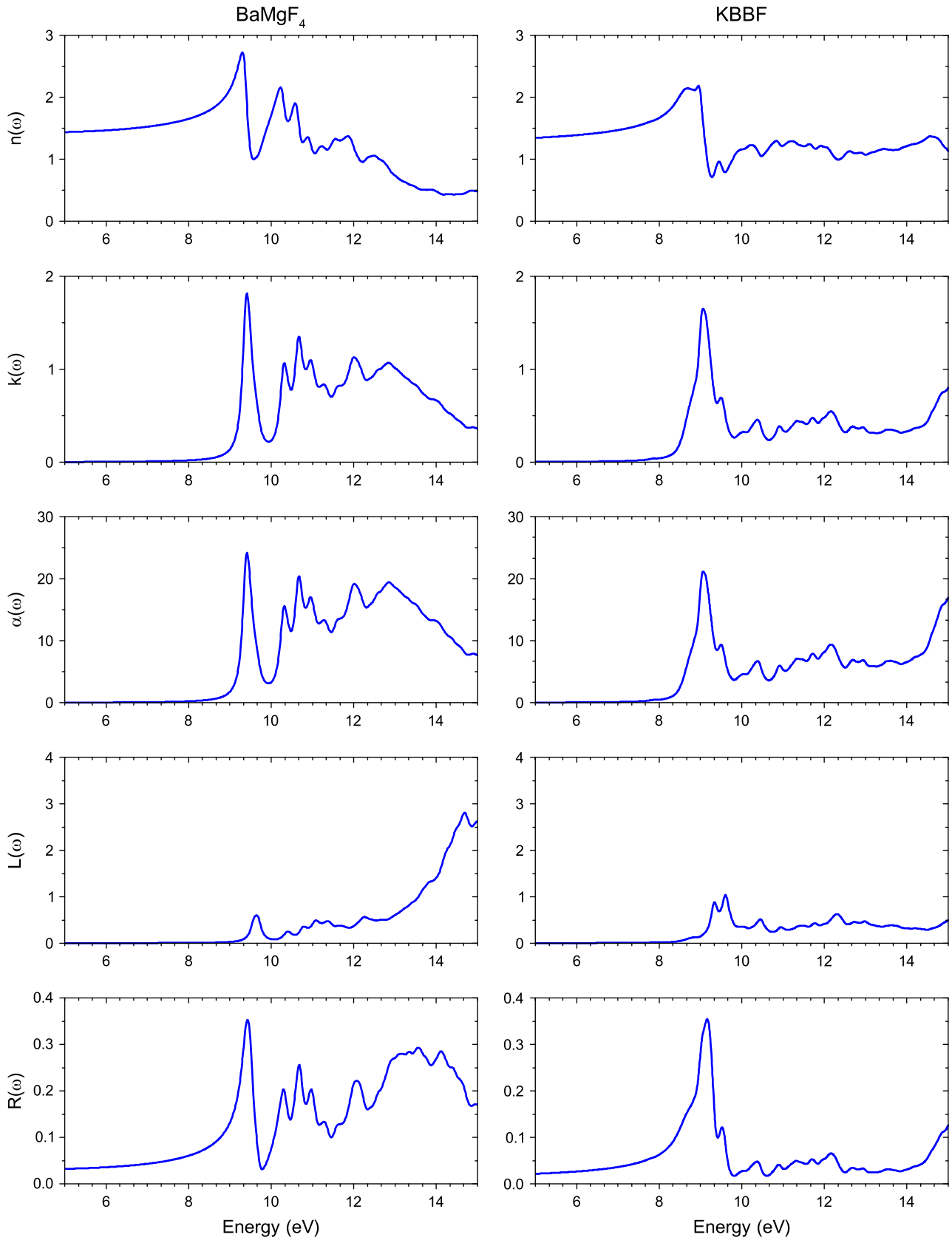

Fig. 6. (Color online) Other frequency-dependent optical properties (e.g., refractive index $n(\omega)$, excitation coefficient $k(\omega)$, absorption coefficient $\alpha(\omega)$, energy-loss function $L(\omega)$, and reflectivity $R(\omega)$) based on the calculated dielectric function $\epsilon(\omega)$ at BSE@GW level.

Table 2
Independent elements of the d-tensor (pm/V) of $BaMgF_4$ and KBBF crystals.

Non-linear optical properties	$BaMgF_4$			KBBF
d-tensor	d_{31}	d_{32}	d_{33}	d_{34}
	0.103 (0.021,0.15)	0.016 (0.039,0.36)	0.091 (0.015,0.12)	0.7 (0.76)
EO-tensor	r_{13} 0.83	r_{23} 0.44	r_{33} 1.27	r_{22} 0.62

3.3. Nonlinear optical properties

Besides the linear optical properties, nonlinear optical properties are calculated as well by taking advantage of $2n+1$ theorem. According to the point group theory, the effective second-order nonlinear optical susceptibility d-tensor of $BaMgF_4$ and KBBF have 5 and 2 independent elements respectively. Furthermore, the Kleinman symmetry rule allows us to reduce this tensor to 3 and 1 independent elements, named d_{31}, d_{32}, d_{33} and d_{34}. The calculated elements are given in Table 2. From Table 2, a reasonable agreement between the theoretical and experimental values was obtained. The divergence may result from two factors. Firstly, the magnitude of $BaMgF_4$ crystal is relatively small compared to usual NLO crystals, which make the experiment particular difficult to measure. We can see that the values reported by different experiment are in substantial disagreement; secondly, our nonlinear optical properties calculations are based on the wavefunctions of DFT level calculations, the impact of energy band corrections are not taken into account in the following calculations which may result in the divergence. As we obtained the second-order nonlinear optical susceptibility, all the elements that needed to calculate the EO tensor, which describe the dependence of the optical dielectric tensor on the static(or low-frequency) electric filed, are available. With the same procedure as second-order nonlinear optical susceptibility, the calculated values are listed in Table 2 as well.

4. Summary

In summary, results concerning the electronic and optical properties of DUV nonlinear optical crystal $BaMgF_4$ and KBBF are presented by means of the many-body Green's function method. In order to obtain the well described band gap, which is crucial for prediction of the performance of DUV crystals in DUV region, QP self-energy corrections to DFT eigenvalues are calculated with the *GW* approximation. *Electronic* band gaps of 10.36 eV and 8.93 eV are determined for $BaMgF_4$ and KBBF crystals. By solving the BSE on top of *GW* approximation, optical absorption spectra and related optical properties of both crystal were calculated. *Optical* band gaps are determined for both crystals, which are 9.26 eV and 7.84 eV, in good agreement with experimental results. By comparing the result with and without *e–h* interaction, we found that both crystal have strong excitonic effects, which are missing in previous studies. Since our study is independent of the experiment, we pave the way that use first-principle theory as a tool to assist the crystal engineering.

Acknowledgments

This research was supported by the National Natural Science Foundation of China (Grant nos. 61235009, 61125503), the National Basic Research Program 973 of China (Grant no. 2011CB808101), and the Foundation for Development of Science and Technology of Shanghai (Grant no. 13JC1408300).

References

[1] S.C. Buchter, T.Y. Fan, V. Liberman, J.J. Zayhowski, M. Rothschild, E.J. Mason, A. Cassanho, H.P. Jenssen, J.H. Burnett, Opt. Lett. 26 (November (21)) (2001) 1693–1695, URL ⟨http://ol.osa.org/abstract.cfm?URI=ol-26-21-1693⟩.
[2] C. Chen, Opt. Mater. 26 (4) (2004) 425–429, Third International Symposium on Lasers and Nonlinear Optical Materials (ISLNOM-3). URL ⟨http://www.sciencedirect.com/science/article/pii/S0925346704000813⟩.
[3] C. Chen, J. Lu, T. Togashi, T. Suganuma, T. Sekikawa, S. Watanabe, Z. Xu, J. Wang, Opt. Lett. 27 (April (8)) (2002) 637–639, URL ⟨http://ol.osa.org/abstract.cfm?URI=ol-27-8-637⟩.
[4] J. Chen, X. Chen, A. Wu, H. Li, Y. Zheng, Y. Ma, L. Jiang, J. Xu, Appl. Phys. Lett. 98 (May (19)) (2011) 191102–191102–3.
[5] X. Gonze, J.-M. Beuken, R. Caracas, F. Detraux, M. Fuchs, G.-M. Rignanese, L. Sindic, M. Verstraete, G. Zerah, F. Jollet, M. Torrent, A. Roy, M. Mikami, P. Ghosez, J.-Y. Raty, D. Allan, Comput. Mater. Sci. 25 (3) (2002) 478–492, URL ⟨http://www.sciencedirect.com/science/article/pii/S0927025602003257⟩.
[6] J. Heyd, G.E. Scuseria, M. Ernzerhof, J. Chem. Phys. 118 (18) (2003) 8207–8215, URL ⟨http://scitation.aip.org/content/aip/journal/jcp/118/18/10.1063/1.1564060⟩.
[7] H. Huang, Z. Lin, L. Bai, R. He, C. Chen, Solid State Commun. 150 (47–48) (2010) 2318–2321, URL ⟨http://www.sciencedirect.com/science/article/pii/S0038109810006009⟩.
[8] T. Kanai, T. Kanda, T. Sekikawa, S. Watanabe, T. Togashi, C. Chen, C. Zhang, Z. Xu, J. Wang, J. Opt. Soc. Am. B 21 (February (2)) (2004) 370–375, URL ⟨http://josab.osa.org/abstract.cfm?URI=josab-21-2-370⟩.
[9] L. Kang, S. Luo, H. Huang, T. Zheng, Z.S. Lin, C.T. Chen, J. Phys.: Condens. Matter 24 (33) (2012) 335503, URL ⟨http://stacks.iop.org/0953-8984/24/i=33/a=335503⟩.
[10] T. Kiss, F. Kanetaka, T. Yokoya, T. Shimojima, K. Kanai, S. Shin, Y. Onuki, T. Togashi, C. Zhang, C.T. Chen, S. Watanabe, Phys. Rev. Lett. 94 (February) (2005) 057001, URL ⟨http://link.aps.org/doi/10.1103/PhysRevLett.94.057001⟩.
[11] Z. Lin, L. Kang, T. Zheng, R. He, H. Huang, C. Chen, Comput. Mater. Sci. 60 (0) (2012) 99–104, URL ⟨http://www.sciencedirect.com/science/article/pii/S0927025612001735⟩.
[12] Z. Lin, Z. Wang, C. Chen, S.K. Chen, M.-H. Lee, Chem. Phys. Lett. 367 (5–6) (2003) 523–527, URL ⟨http://www.sciencedirect.com/science/article/pii/S0009261402017281⟩.
[13] A. Marini, C. Hogan, M. Grüning, D. Varsano, Comput. Phys. Commun. 180 (8) (2009) 1392–1403, URL ⟨http://www.sciencedirect.com/science/article/pii/S0010465509000472⟩.
[14] H.J. Monkhorst, J.D. Pack, Phys. Rev. B 13 (June) (1976) 5188–5192, URL ⟨http://link.aps.org/doi/10.1103/PhysRevB.13.5188⟩.
[15] G. Onida, L. Reining, A. Rubio, Rev. Mod. Phys. 74 (June) (2002) 601–659, URL ⟨http://link.aps.org/doi/10.1103/RevModPhys.74.601⟩.
[16] J.P. Perdew, Y. Wang, Phys. Rev. B 45 (June) (1992) 13244–13249, URL ⟨http://link.aps.org/doi/10.1103/PhysRevB.45.13244⟩.
[17] V. Petrov, F. Rotermund, F. Noack, R. Komatsu, T. Sugawara, S. Uda, J. Appl. Phys. 84 (December (11)) (1998) 5887–5892.
[18] C.A. Rozzi, D. Varsano, A. Marini, E.K.U. Gross, A. Rubio, Phys. Rev. B 73 (May) (2006) 205119, URL ⟨http://link.aps.org/doi/10.1103/PhysRevB.73.205119⟩.
[19] F. Seifert, J. Ringling, F. Noack, V. Petrov, O. Kittelmann, Opt. Lett. 19 (October (19)) (1994) 1538–1540, URL ⟨http://ol.osa.org/abstract.cfm?URI=ol-19-19-1538⟩.
[20] M. Shishkin, M. Marsman, G. Kresse, Phys. Rev. Lett. 99 (December) (2007) 246403, URL ⟨http://link.aps.org/doi/10.1103/PhysRevLett.99.246403⟩.
[21] T. Togashi, T. Kanai, T. Sekikawa, S. Watanabe, C. Chen, C. Zhang, Z. Xu, J. Wang, Opt. Lett. 28 (February (4)) (2003) 254–256, URL ⟨http://ol.osa.org/abstract.cfm?URI=ol-28-4-254⟩.
[22] N. Troullier, J.L. Martins, Phys. Rev. B 43 (January) (1991) 1993–2006, URL ⟨http://link.aps.org/doi/10.1103/PhysRevB.43.1993⟩.
[23] M. van Schilfgaarde, T. Kotani, S. Faleev, Phys. Rev. Lett. 96 (June) (2006) 226402, URL ⟨http://link.aps.org/doi/10.1103/PhysRevLett.96.226402⟩.
[24] M. Veithen, X. Gonze, P. Ghosez, Phys. Rev. Lett. 93 (October) (2004) 187401, URL ⟨http://link.aps.org/doi/10.1103/PhysRevLett.93.187401⟩.
[25] M. Veithen, X. Gonze, P. Ghosez, Phys. Rev. B 71 (March) (2005) 125107, URL ⟨http://link.aps.org/doi/10.1103/PhysRevB.71.125107⟩.
[26] E.G. Víllora, K. Shimamura, K. Sumiya, H. Ishibashi, Opt. Express 17 (July (15)) (2009) 12362–12378, URL ⟨http://www.opticsexpress.org/abstract.cfm?URI=oe-17-15-12362⟩.
[27] W. Zhang, G. Liu, L. Zhao, H. Liu, J. Meng, X. Dong, W. Lu, J.S. Wen, Z.J. Xu, G. D. Gu, T. Sasagawa, G. Wang, Y. Zhu, H. Zhang, Y. Zhou, X. Wang, Z. Zhao, C. Chen, Z. Xu, X.J. Zhou, Phys. Rev. Lett. 100 (March) (2008) 107002, URL ⟨http://link.aps.org/doi/10.1103/PhysRevLett.100.107002⟩.